

Ocean Color through AEOLUS measurements: results from the COLOR project

D. Dionisi¹, S. Bucci², C. Cesarini¹, S. Colella¹, D. D'Alimonte³, L. Di Ciolo², P. Di Girolamo⁴, M. Di Paolantonio¹, N. Franco⁴, G. Gostinicchi², T. Kajiyama³, G. L. Liberti¹, E. Organelli¹, R. Santoleri¹

Consortium:

- 1 - Consiglio Nazionale delle Ricerche, Istituto di Scienze Marine, Rome, Italy
- 2 - Serco Italia S.p.A., Frascati, Italy
- 3 - AEQUORA, Lisbon, Portugal
- 4 - Università degli Studi della Basilicata, Potenza, Italy



COLOR

CDOM-proxy retrieval from aeOLus ObseRvations

➤ Introduction

- 1- Scientific context
- 2- COLOR overview

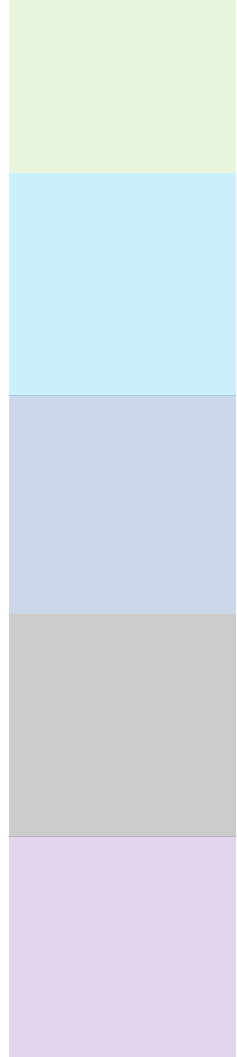
➤ Methods

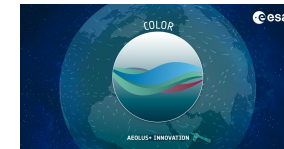
- 1- LiOC in-water forward model
- 2- AEOLUS in-water algorithm

➤ Results

- 1- Statistical assessment
- 2- Match-up assessment

➤ Roadmap and conclusions





COLOR

CDOM-proxy retrieval from aeOLus ObseRvations

➤ Introduction

- 1- Scientific context
- 2- COLOR overview

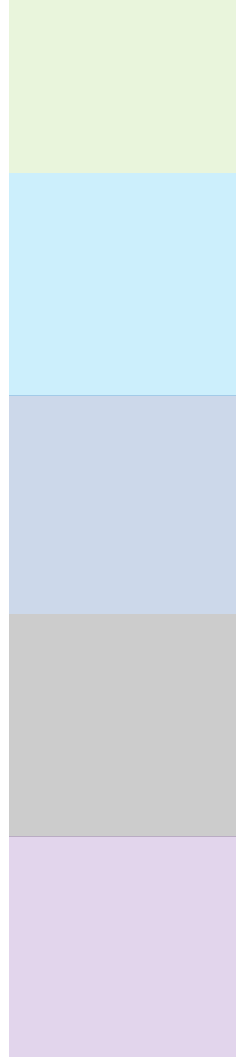
➤ Methods

- 1- LiOC in-water forward model
- 2- AEOLUS in-water algorithm

➤ Results

- 1- Statistical assessment
- 2- Match-up assessment

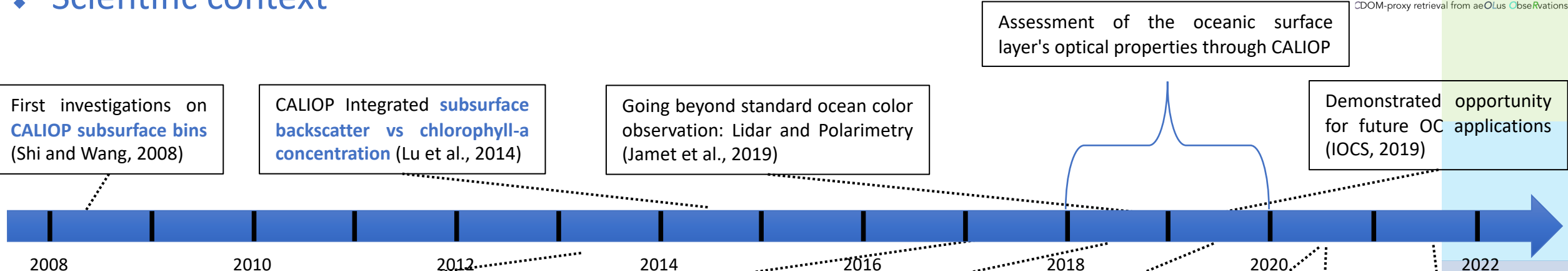
➤ Roadmap and conclusions



Introduction



❖ Scientific context



First investigations on **CALIOP subsurface bins** (Shi and Wang, 2008)

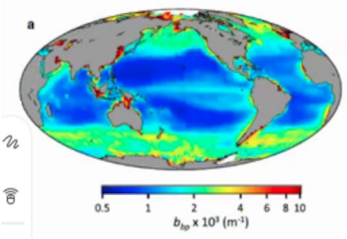
CALIOP Integrated **subsurface backscatter vs chlorophyll-a concentration** (Lu et al., 2014)

Going beyond standard ocean color observation: Lidar and Polarimetry (Jamet et al., 2019)

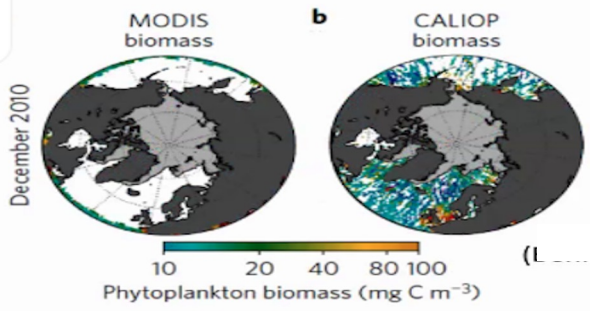
Assessment of the oceanic surface layer's optical properties through CALIOP

Demonstrated opportunity for future OC applications (IOCS, 2019)

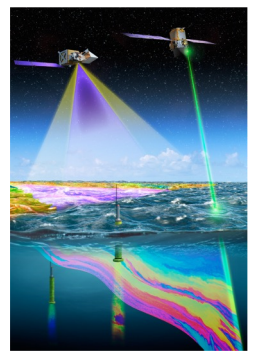
Ocean particulate backscatter from Caliop



Annual cycle of polar phytoplankton **biomass**



New **lidar era** in satellite oceanography (Hostetler et al., 2018)



Ocean subsurface observations through ICESat-2 (Lu et al., 2019)

CALIOP δ_T used as an oceanic variable for the ocean particulate optical properties (Dionisi et al., 2020)

Vertical distribution of phytoplankton optical properties through CALIOP and ICESat-2 measurements (Lu et al., 2021)

GUANLAN mission for space oceanography (S. Wu, Aeolus cal/val meeting, 2020)

Satellite lidars can complement passive ocean color data

❖ Scientific context

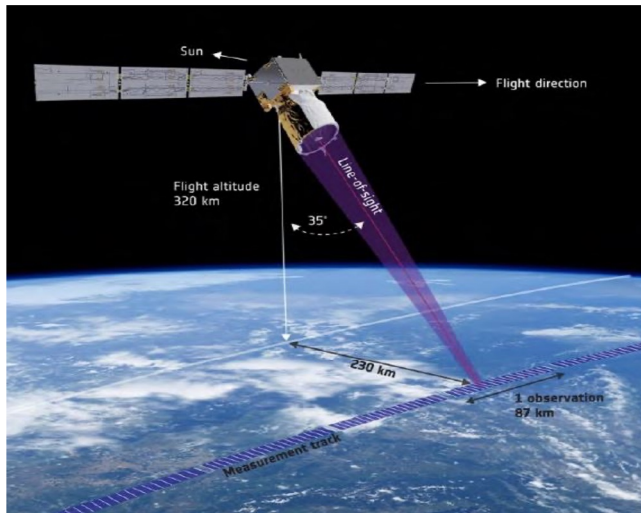
In the **ocean**, at 355 nm:

- b_b (sub-surface hemispheric backscatter coefficient) dominated by the contribution due to water molecules
- K_d (diffuse attenuation coefficient for downwelling irradiance) dominated by light absorption of optically-significant water constituents (water, particles and CDOM)

Chromophoric Dissolved Organic Matter (**CDOM**) is the most relevant contributor to the light absorption at 355 nm. In the UV, K_d can be assumed as a proxy of CDOM light absorption

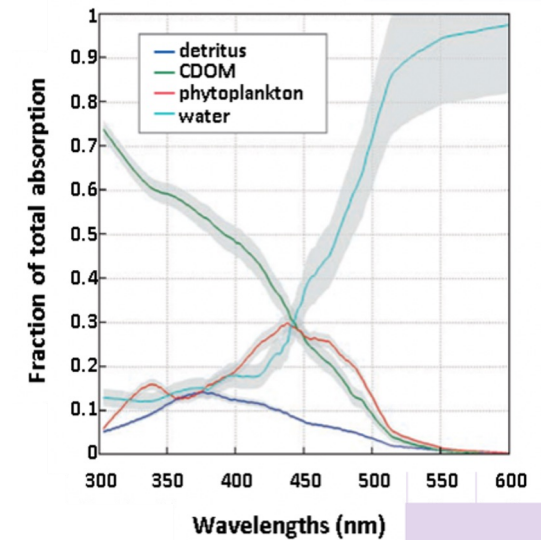
CDOM has high relevance in the ocean-climate system (e.g. tracer of physical and biogeochemical processes, ocean carbon cycle, absorption of solar radiation, source of uncertainty for ocean color chlorophyll algorithm)

Lack of the UV information of past and current Ocean Color sensors



AEOLUS gives the opportunity to investigate the signal backscattered by the ocean sub-surface:

- ❑ First orbiting HSRL lidar
- ❑ Ocean subsurface information content in the UV
- ❑ The line-of-sight (LOS) points 35° from nadir



❖ COLOR overview

COLOR (*CDOM-proxy retrieval from aeOLus ObseRvations*) is an on-going 18 month feasibility study approved by **ESA** within the **Aeolus+ Innovation program** (ESA AO/1-9544/20/I/NS). **End: April 2023.**

Objective

COLOR proposes to evaluate and document the **feasibility** of deriving an **in-water AEOLUS product** at 355 nm (lidar attenuation coefficient K_L , in-water backscattering β_{wat} → ocean color parameters, e.g. K_d , Chl-a, CDOM)

Consortium



Institute of Marine Sciences
(ISMAR) - CNR



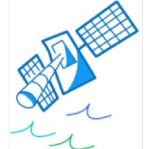
University of Basilicata



Aequora



Serco Italia SpA



COLOR
CDOM-proxy retrieval from aeOLus ObseRvations

COLOR

CDOM-proxy retrieval from aeOLus ObseRvations

➤ Introduction

- 1- Scientific context
- 2- COLOR overview

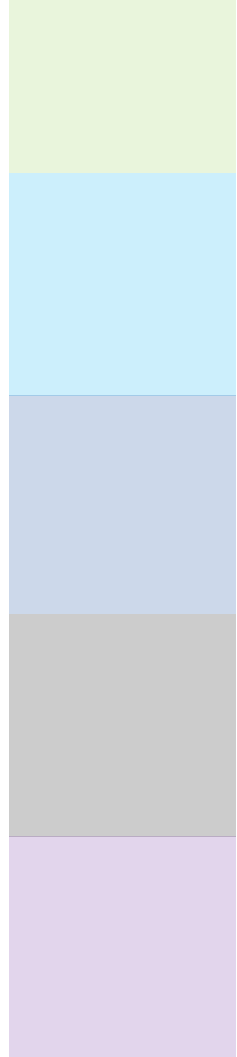
➤ Methods

- 1- LiOC in-water forward model
- 2- AEOLUS in-water algorithm

➤ Results

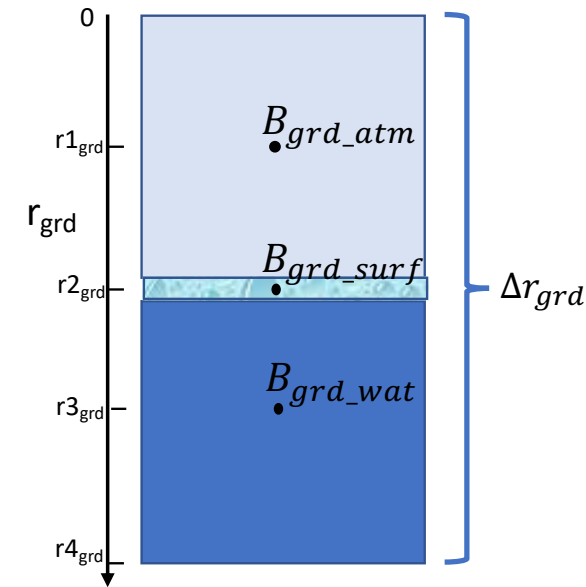
- 1- Statistical assessment
- 2- Match-up assessment

➤ Roadmap and conclusions



❖ General approach: ground bin characterization

The potential information on ocean subsurface optical properties is contained in the AEOLUS ground bin volume (Δr_{grd})



$$S_X(grd) = M_X \left[\frac{A}{\left(r_{atm} + \frac{\Delta r_{atm}}{n} \right)^2} B_{grd} T_A^2(r_{atm}) + S_{bkd} \right] \quad (1)$$

$X = Ray_{A,B}$
 $X = Mie$

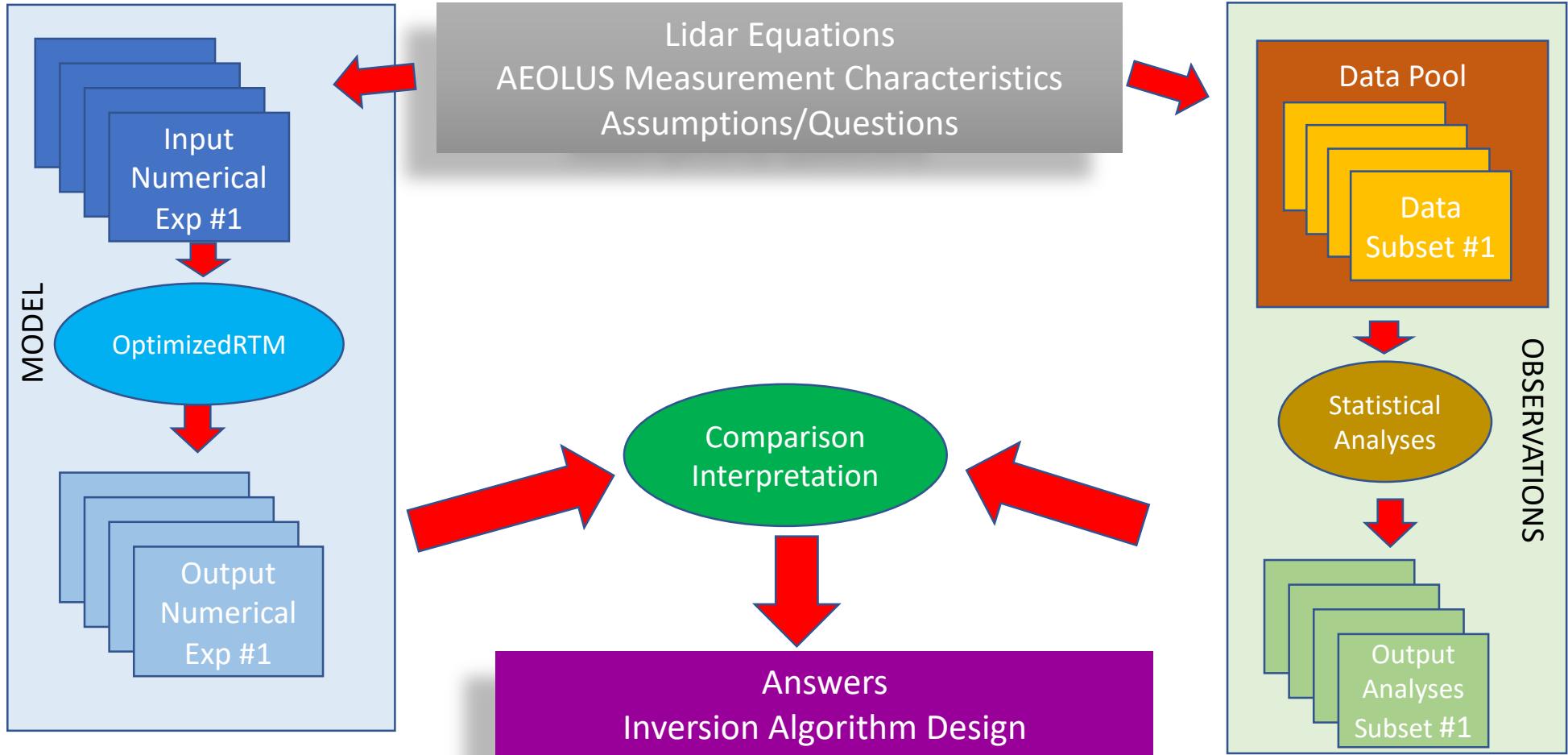
$$B_{grd} = B_{atm} + B_{srf} + B_{wat}(K_L, \beta_{wat}^{par}, \beta_{wat}^{mol}) \quad (2)$$

$$B_{wat} = \int_0^{r_{wat}} \beta_{wat}(\pi, r'_{wat}) \exp \left[-2 \int_0^{r'_{wat}} K_{LID}(r''_{wat}) dr''_{wat} \right] dr'_{wat} \quad (3)$$

This characterization is based on:

- a) Radiative transfer numerical modelling
- b) AEOLUS data analysis

❖ General approach: ground bin characterization



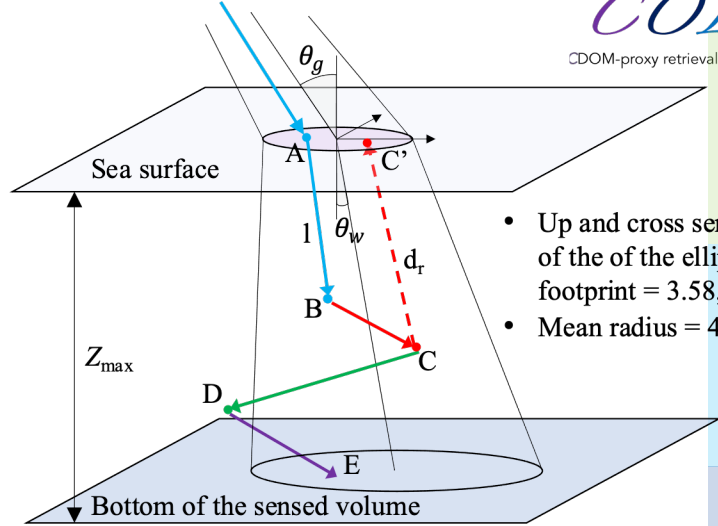
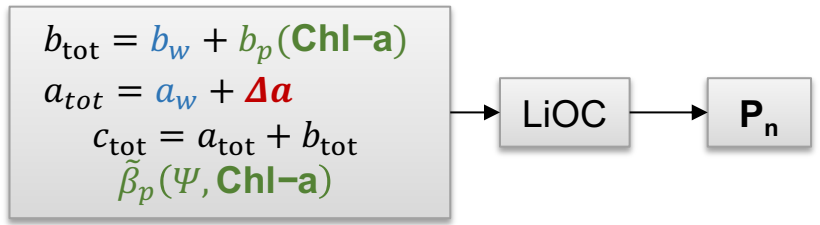
LiOC in-water forward model

Lidar simulation code for Ocean Color applications (**LiOC**) developed fully accounting for ALADIN characteristics for two main tasks:

- ❑ understand the lidar dynamics
- ❑ create an inversion scheme to retrieve in-water optical properties

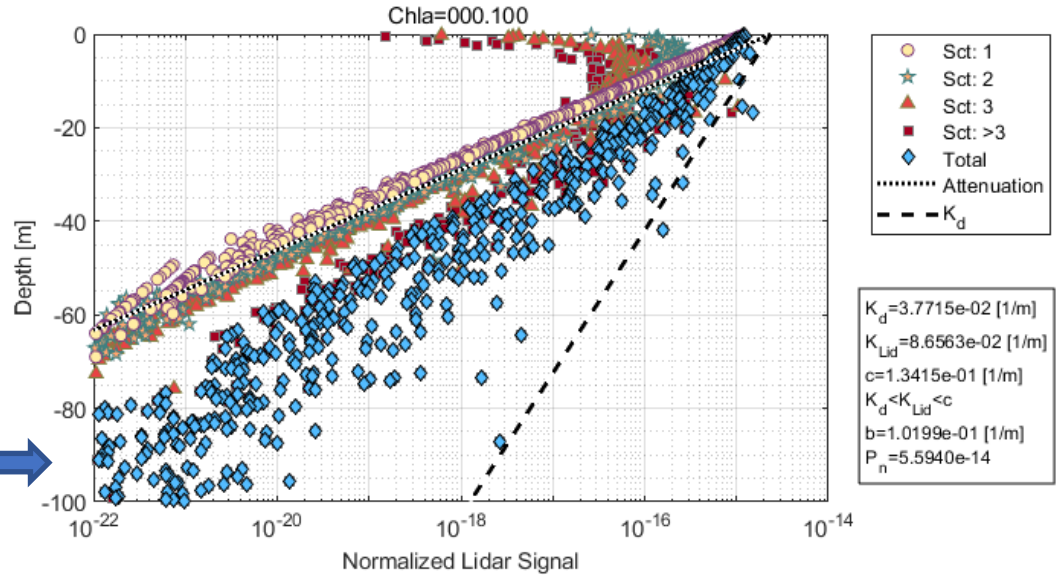
LiOC components: $P_n = P_n^s + P_n^b + P_n^w$

- At the surface: negligible contribution of the reflected signal for wind speed up to the formation of white caps ($\sim 8 \text{ ms}^{-1}$)
- At the bottom: negligible contribution of bottom effects in oligotrophic conditions for depth $\leq 80 \text{ m}$.
- In the water columns: MC ray tracing is driven by seawater Inherent Optical Properties.



- Up and cross semi-axis of the of the ellipse footprint = 3.58, 4.49 [m]
- Mean radius = 4.03 [m]

Ray-tracing scheme



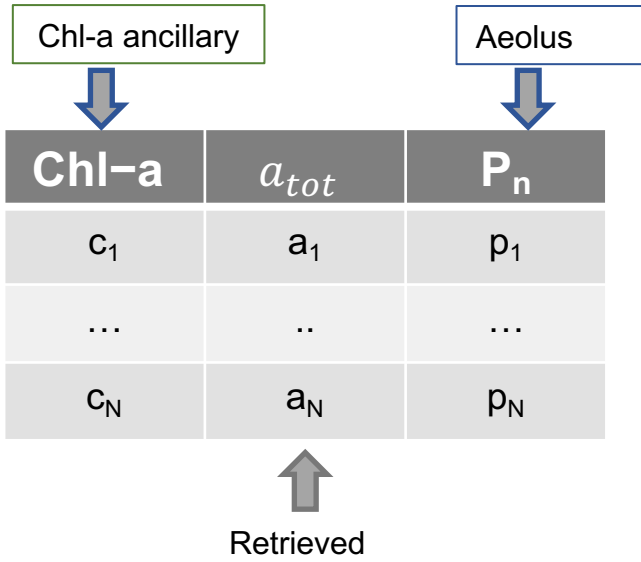
LiOC in-water forward model

Overview of the backward scheme for a_{tot} retrieval

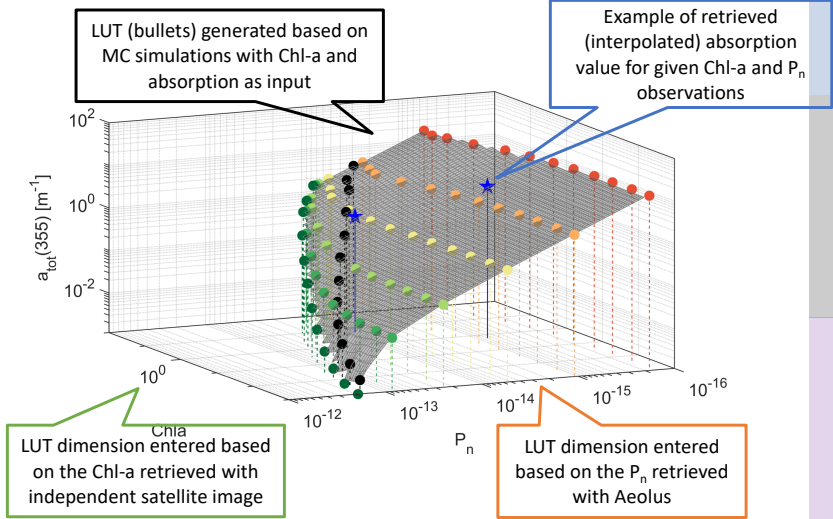
1. LUT was computed through forward MC simulations to determine P_n as a function of IOPs.
2. The LUT is entered through the observed **Chl-a** and P_n values
3. The a_{tot} value is retrieved by interpolation

Δa log-uniformly varied between 0 and $15 m^{-1}$

Chl-a	Δa log-uniformly varied between 0 and $15 m^{-1}$												Ref. case	
	Pn	a1	Pn	a2	Pn	a3	Pn	a4	Pn	a5	Pn	a6	Pn	atot
0.001	1.92E-13	0.0012	8.48E-14	0.0212	2.49E-14	0.1012	5.39E-15	0.5012	1.09E-15	2.5012	1.82E-16	15.0012	1.83E-13	0.0025
0.003	1.75E-13	0.0014	8.19E-14	0.0214	2.49E-14	0.1014	5.43E-15	0.5014	1.10E-15	2.5014	1.83E-16	15.0014	1.54E-13	0.0041
0.01	1.46E-13	0.0021	7.73E-14	0.0221	2.49E-14	0.1021	5.49E-15	0.5021	1.11E-15	2.5021	1.86E-16	15.0021	1.18E-13	0.0078
0.03	1.20E-13	0.0037	6.98E-14	0.0237	2.48E-14	0.1037	5.62E-15	0.5037	1.14E-15	2.5037	1.91E-16	15.0037	8.62E-14	0.015
0.1	9.10E-14	0.0078	6.17E-14	0.0278	2.47E-14	0.1078	5.87E-15	0.5078	1.19E-15	2.5078	2.00E-16	15.0078	5.61E-14	0.0322
0.3	6.84E-14	0.0168	5.16E-14	0.0368	2.40E-14	0.1168	6.10E-15	0.5168	1.27E-15	2.5168	2.14E-16	15.0168	3.60E-14	0.0658
1	4.82E-14	0.0408	3.98E-14	0.0608	2.21E-14	0.1408	6.71E-15	0.5408	1.42E-15	2.5408	2.41E-16	15.0408	2.23E-14	0.146
3	3.49E-14	0.0934	2.96E-14	0.1134	2.04E-14	0.1934	7.11E-15	0.5934	1.68E-15	2.5934	2.87E-16	15.0934	1.33E-14	0.3047
10	2.33E-14	0.2334	2.12E-14	0.2534	1.61E-14	0.3334	7.70E-15	0.7334	2.19E-15	2.7334	3.90E-16	15.2334	8.19E-15	0.6873
30	1.51E-14	0.5405	1.42E-14	0.5605	1.23E-14	0.6405	7.65E-15	1.0405	2.69E-15	3.0405	4.88E-16	15.5405	5.08E-15	1.4524
100	7.62E-15	1.3586	7.18E-15	1.3786	6.65E-15	1.4586	5.27E-15	1.8586	2.33E-15	3.8586	5.40E-16	16.3586	2.91E-15	3.3173



$$P_N = B_{wat} \cdot \Delta\Omega_r$$

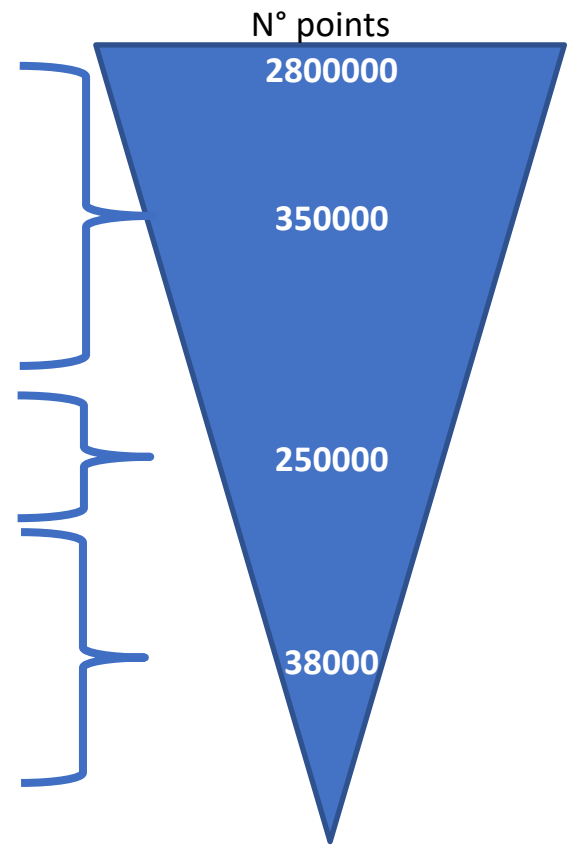


❖ Data screening

AEOLUS data L1B; IB11; Apr2020 – Mar2021

Measurement resolution (averaged over 20 to 50 laser pulses, i.e. horizontal length of 3 km to 7 km)

Flag	Bit
Dummy value (bin 21)	1
Dummy value (bin 22)	2
Dummy value (bin 23)	3
Shallow water bin	4
Deep water bin	5
Bathymetry	6
High wind	7
Low SNR on Mie channel (bin 21)	8
Low SNR on Mie channel (bin 22)	9
Low SNR on Mie channel (bin 23)	10
High SNR on Mie channel (bin 21)	11
High SNR on Mie channel (bin 22)	12
High SNR on Mie channel (bin 23)	13
Cloud/Aerosol Contamination (bin 21)	14
Cloud/Aerosol Contamination (bin 22)	15
Cloud/Aerosol Contamination (bin 23)	16



Removal of the majority of cloud contaminated bins but filtering out around 99% of the original data sample.

❖ AEOLUS in-water algorithm

High Spectral Resolution Lidar approach

Objective: coupling the signals coming from Brillouin and Mie spectra (Rayleigh+Mie channels)



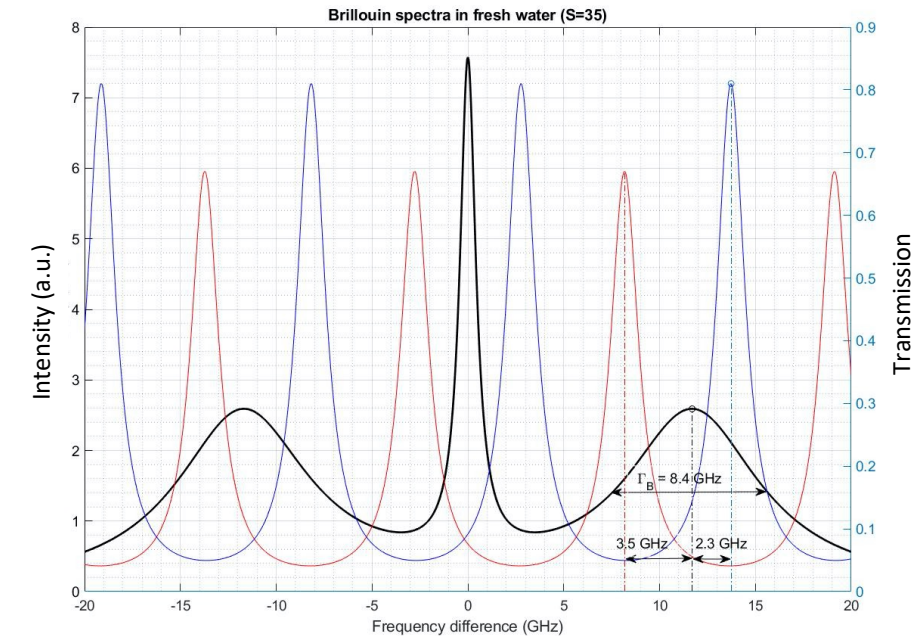
HSRL in water

$$S_{Mie} = M_{Mie}^w \left[\frac{A}{\left(r_{atm} + \frac{\Delta r_{atm}}{n}\right)^2} \right] (C_4^w \beta_{wat}^m + C_3^w \beta_{wat}^p) \exp \left[-2 \int_0^{r_{wat}} K_{LID}(r'_{wat}) dr'_{wat} \right] T_A^2(r_{atm})$$

$$S_{Ray} = M_{Ray}^w \left[\frac{A}{\left(r_{atm} + \frac{\Delta r_{atm}}{n}\right)^2} \right] (C_1^w \beta_{wat}^m + C_2^w \beta_{wat}^p) \exp \left[-2 \int_0^{r_{wat}} K_{LID}(r'_{wat}) dr'_{wat} \right] T_A^2(r_{atm})$$

$$\beta_{wat}^p = \beta_{wat}^m \left[\frac{S_R M_{Mie}^w C_4^w - M_{Ray}^w C_1^w}{M_{Ray}^w C_2^w - S_R M_{Mie}^w C_3^w} \right]$$

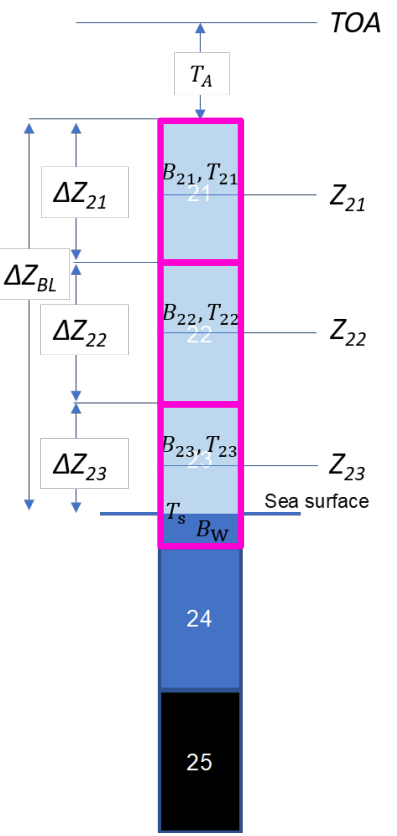
- Calibration and cross talk coefficients estimated for atmospheric application **cannot be used for the Brillouin scattering in water**
- High variability of the Rayleigh ground bin signal



FWHM	1,78 GHz
FSR	10,95 GHz
Spacing between A and B	5,5 GHz
Filter A Peak Transmission	81 %
Filter B Peak Transmission	67 %

❖ AEOLUS in-water algorithm

Elastic Backscatter Lidar AEOLUS-adapted inversion algorithm



Rationale is to use the information in bins 21 and 22 to account for the contribution due to the instrument characteristics and to the atmosphere in the bin 23 signal

INPUTS: (Mie channel) Range Corrected Signals (S_{xx}^*) and geometry of bins 21, 22, 23 ($z_{xx}, \Delta z_{xx}$)

ANCILLARY: Atmospheric density profile, surface wind (T_s^2), sea temperature and salinity, aerosols scale height (z_s).

OUTPUT: sea water contribution (backscattering+extinction) to ground bin signal (B_w)

$$S_{21}^* = C B_{21} T_A^2$$

$$S_{22}^* = C B_{22} T_A^2 T_{21}^2$$

$$S_{23}^* = \frac{C}{n^2} B_w T_s^2 T_A^2 T_{21}^2 T_{22}^2 T_{23}^2 + C B_{23} T_A^2 T_{21}^2 T_{22}^2$$

$$B_{wat} \approx \frac{(S_{23}^* - S_{22}^*)}{S_{21}^*} \frac{B_{21m} n^2}{T_s^2 T_{BLm}^2} e^{\left(\frac{2\rho_0 \sigma_{ext}}{\cos \theta} \left(e^{\frac{-z_{21}}{z_s} \Delta z_{21}} + e^{\frac{-z_{22}}{z_s} \Delta z_{22}} + e^{\frac{-z_{23}}{z_s} \Delta z_{23}} \right) \right)}$$

where: $\frac{2\rho_0 \sigma_{ext}}{\cos \theta} \approx -\ln \left(\frac{B_{21m}}{B_{22m}} \frac{1}{T_{21m}^2} \frac{S_{22}^*}{S_{21}^*} \right) \frac{z_{21}}{\Delta z_{21}}$

❖ AEOLUS in-water algorithm

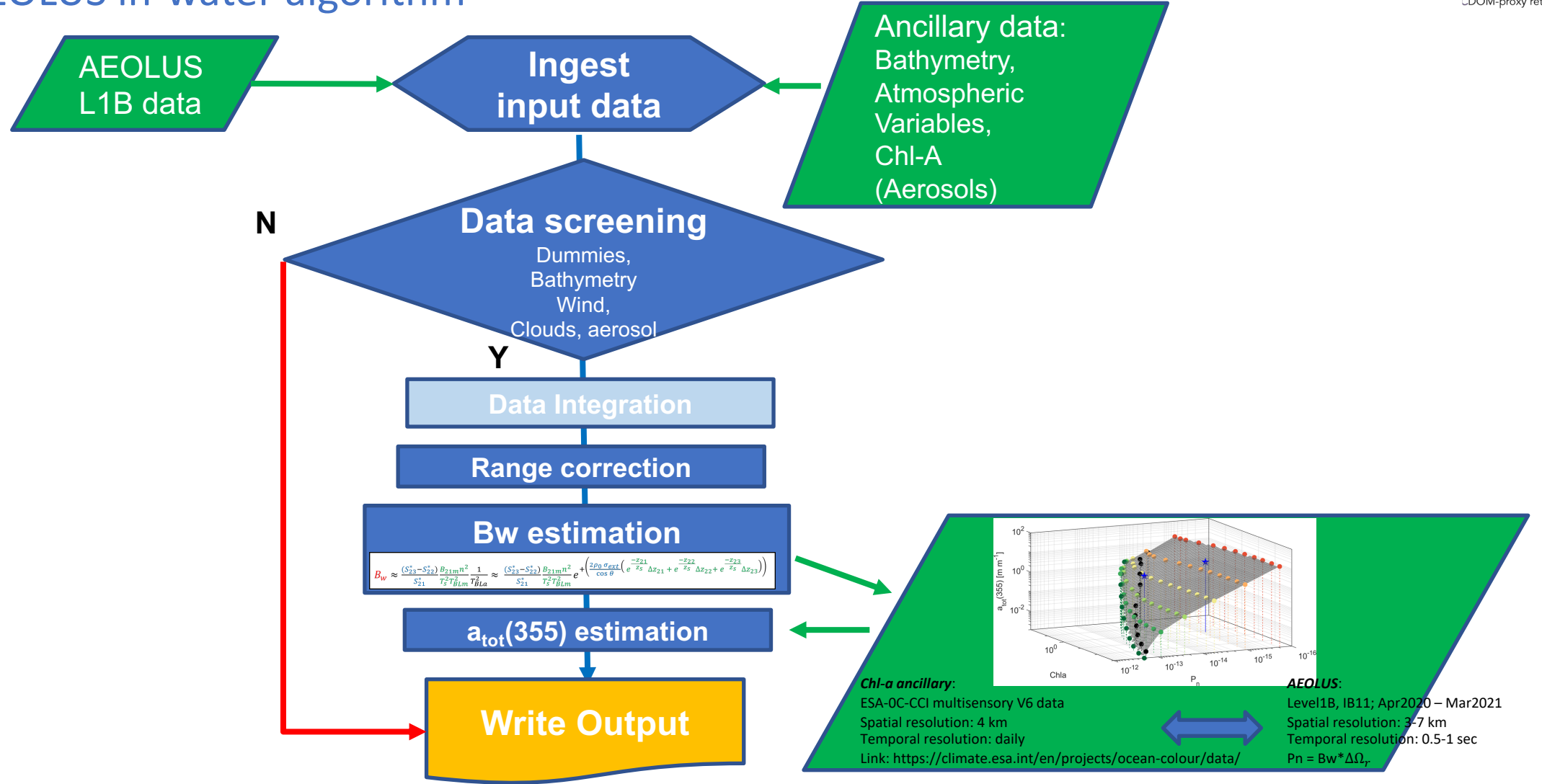
EBL AEOLUS-adapted inversion algorithm

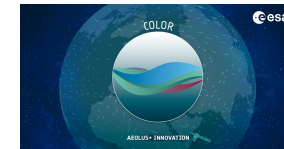
$$B_{wat} \approx \frac{(S_{23}^* - S_{22}^*)}{S_{21}^*} \frac{B_{21m} n^2}{T_s^2 T_{BLm}^2} \frac{1}{T_{BLa}^2} \approx \frac{(S_{23}^* - S_{22}^*)}{S_{21}^*} \frac{B_{21m} n^2}{T_s^2 T_{BLm}^2} e^{\left(\frac{2\rho_0 \sigma_{ext}}{\cos \theta} \left(e^{\frac{-z_{21}}{z_s} \Delta z_{21}} + e^{\frac{-z_{22}}{z_s} \Delta z_{22}} + e^{\frac{-z_{23}}{z_s} \Delta z_{23}} \right) \right)}$$

ASSUMPTIONS:

- Contributions of **sea surface backscattering** and of **sea bottom reflection** are **negligible**
- sea surface transmittance $T_s = 0.97$, independent from the direction of propagation
- refractive index of sea water $n=1.356$ independent from salinity and temperature
- The **difference** between atmospheric **backscattering contribution of bin 22 and 23** is **negligible** compared to the contribution of **sea water in bin 23**
- Atmospheric backscattering dominated by molecular contribution both for the optical thickness as well as for the shape of the phase function;
- **Homogeneity of the aerosol type** in the Marine Atmospheric Boundary Layer (MABL) and **known vertical distribution**

❖ AEOLUS in-water algorithm





COLOR

CDOM-proxy retrieval from aeOLus ObseRvations

➤ Introduction

- 1- Scientific context
- 2- COLOR overview

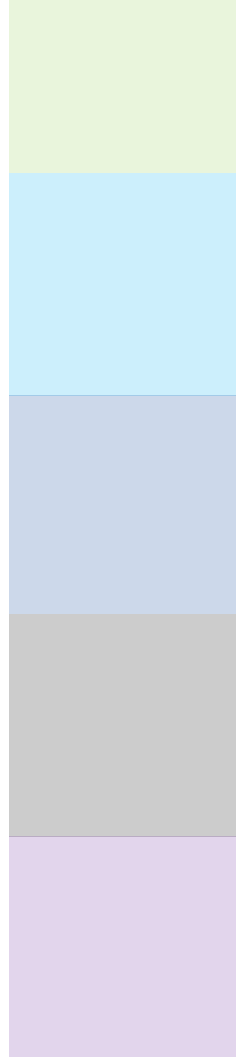
➤ Methods

- 1- LiOC in-water forward model
- 2- AEOLUS in-water algorithm

➤ Results

- 1- Statistical assessment
- 2- Match-up assessment

➤ Roadmap and conclusions



Reference datasets

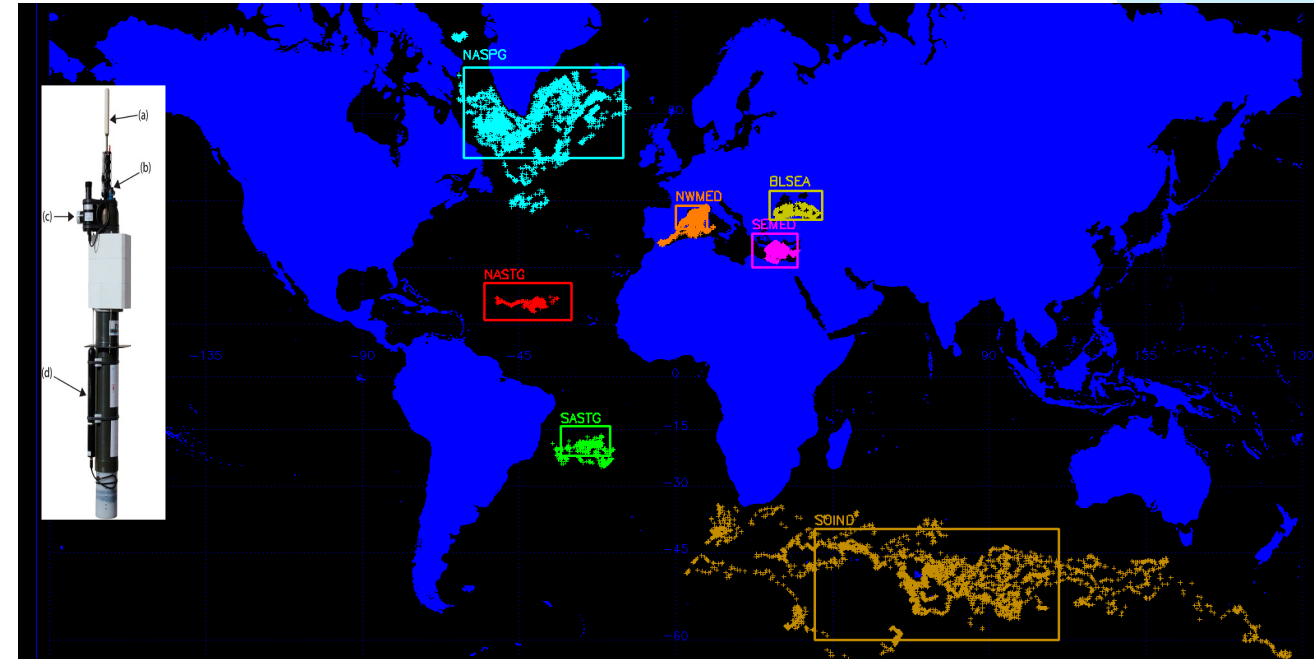
- a) BGC-Argo (global scale; >40000 radiometric profiles at 4 bands available since 2012, <https://maps.biogeochemical-argo.com/bgcargo/>)
- b) ESA Ocean Colour Climate Change Initiative (ESA-OC-CCI; esa-oceancolour-cci.org)

AEOLUS dataset

AEOLUS L1B Dataset, Baseline 11: April 2020 - March 2021.

Regions of Interest

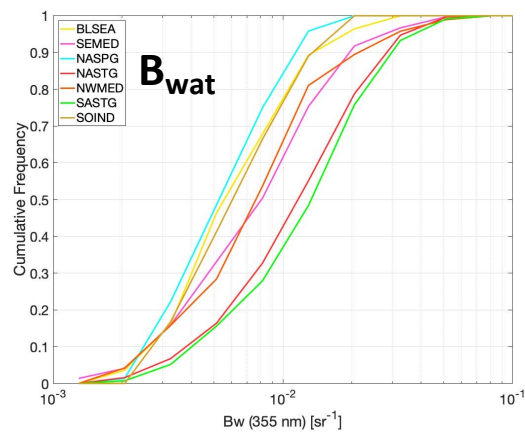
7 regions with different ranges of variability on ocean optical properties



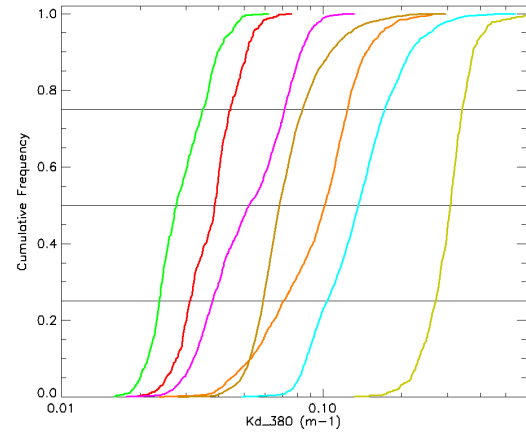


Statistical assessment

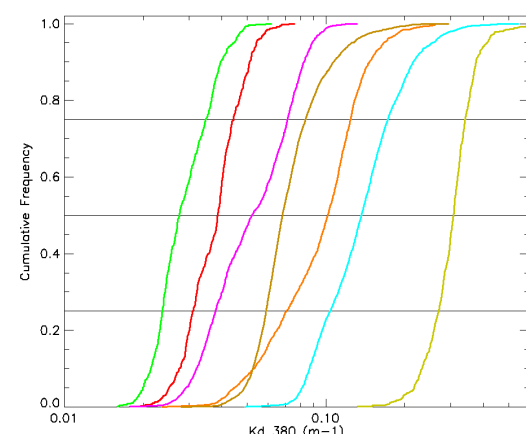
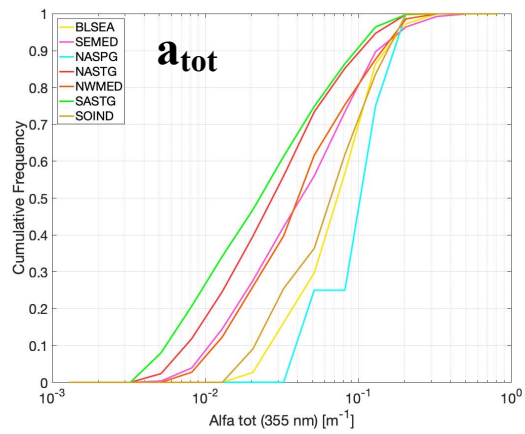
AEOLUS



BGC-ARGO



a_{tot}



Region\Season	DJF	MAM	JJA	SON	ALL
NASTG	544	441	291	487	1763
SASTG	350	263	241	113	967
NWMED	10	6	52	27	95
SEMED	51	55	170	89	365
NASPG	4	19	26	23	72
BLSEA	4	6	32	14	56
SOIND	43	27	58	27	155

- Low number of points for NWMED, BLSEA, NASPG, SOIND
- No statistical significance for seasonal studies
- Good inverse (direct) relationship for B_w (a_{tot})

Region\Season	DJF	MAM	JJA	SON	ALL
NASTG	193	146	127	252	718
SASTG	212	130	140	79	561
NWMED	8	4	44	17	73
SEMED	34	40	144	64	282
NASPG	0	0	3	1	4
BLSEA	1	4	22	10	37
SOIND	24	9	3	19	55

Match-up assessment

Reference dataset

Database: climate.esa.int/en/projects/ocean-colour/data/
 Algorithms: docs.pml.space/share/s/fzNSPb4aQaSDvO7xBNO
[Clw](#) (*a_{dg} pg.33, CHL pg.31*)
 Extracted variables: $a_{dg}@412nm$ (total) (m^{-1})
 Multisensory V6 data (4 km, daily)

$$\Delta a(355) = a_{tot}(355) - a_w(355) - (0.052 \cdot Chl-a^{0.635})$$

$$\Delta a(355) = a_{CDOM}(355) + a_{NAP}(355)$$

$$a_{CDOM}(355) \gg a_{NAP}(355)$$

$$a_{CDOM}(355) \approx \Delta a(355)$$

Match-up criteria

- 1) Temporal matching:** within ± 24 hours time lag between AEOLUS and ESA-OC-CCI
- 2) Spatial matching:** 5x5 pixels (20x20 km) of a_{dg} product selected around the AEOLUS lat-lon measurement.
- 3) Number of valid pixels:** ≥ 4 out of 25 to calculate a_{dg} as the mean value of these pixels.

$$a_{dg}(412) = a_{CDOM}(412) + a_{NAP}(412)$$

$$a_{CDOM}(412) \gg a_{NAP}(412)$$

$$a_{CDOM}(355) \approx a_{dg}(412) \cdot \exp[-0.014(355 - 412)]$$

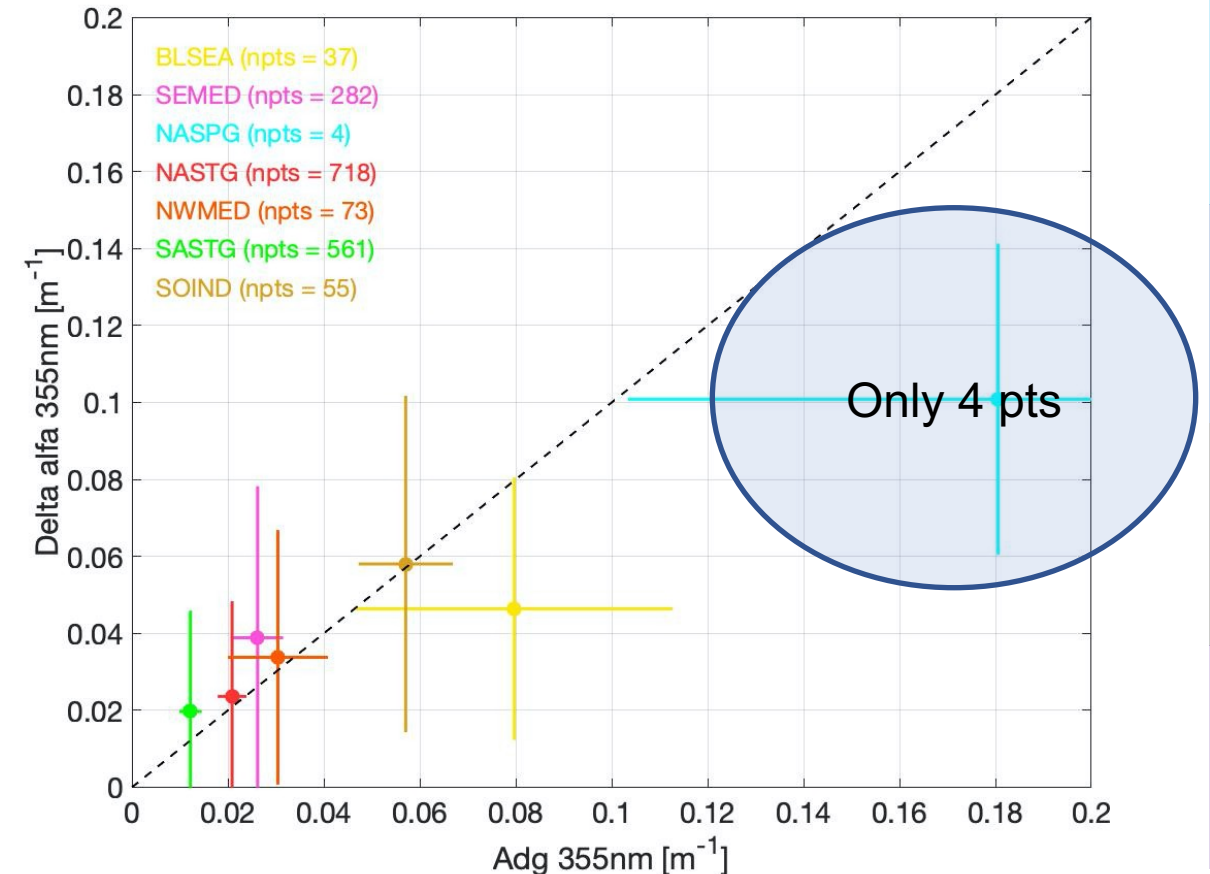
Pitarch et al., 2017

Match-up assessment

- ESA-OC-CCI @ 412 nm scaled @ 355 nm
- Dataset: April 2020 - March 2021
- only AEOLUS data with $\Delta Bw/Bw \leq 1$

- Good agreement for
 - SASTG and NASTG (statistically significant number of match-up pairs)
 - SOIND and NWMED (low number of match-up)
- Δa higher for SEMED than NWMED \rightarrow more than 50% for JJA period (oligotrophic conditions and aerosol dust near the surface)
- Disagreement for BLSEA (different trophic regime, low number of valid match-up)
- NASPG not significant number (4) of match-ups

Statistical (median+interquartile range) comparison due to high variability associated to AEOLUS single values

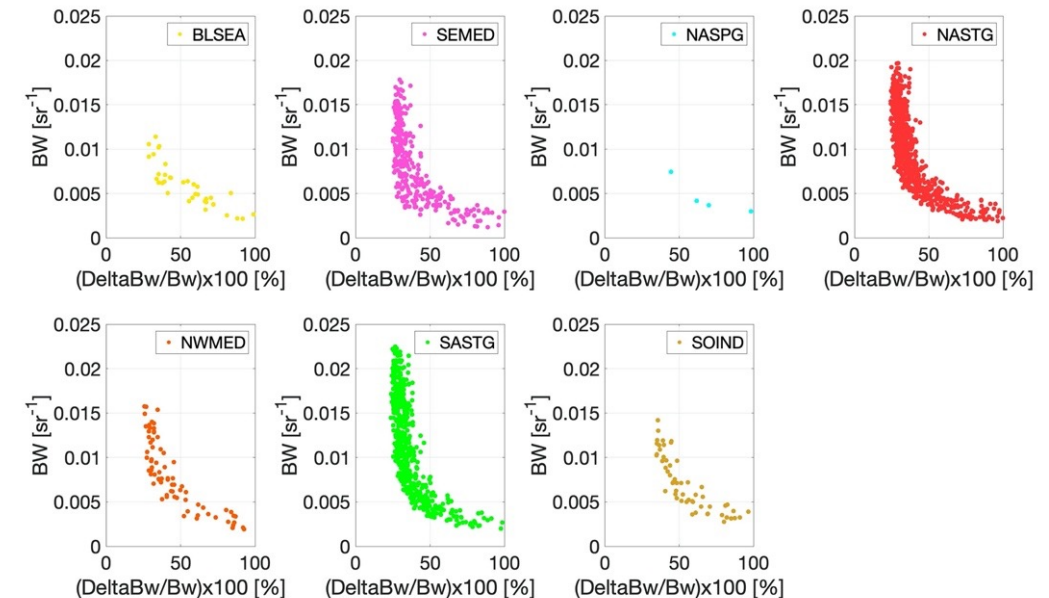


Estimation of associated uncertainty

Identified sources of uncertainties:

- *Data homogeneity*
- *Radiometric noise*
- *Cloud contamination*
- *Assumptions in the analytical model*
- *Aerosols*
- *$B_w \rightarrow \alpha$ conversion*

$$\Delta B_{wat}(355) = \sqrt{\left(\frac{\partial B_w}{\partial S_{21}^*}\right)^2 \cdot (\Delta S_{21}^*)^2 + \left(\frac{\partial B_w}{\partial S_{22}^*}\right)^2 \cdot (\Delta S_{22}^*)^2 + \left(\frac{\partial B_w}{\partial S_{23}^*}\right)^2 \cdot (\Delta S_{23}^*)^2}$$



Associated uncertainty to the prototype product is based on the effect of radiometric noise recognized as major (and quantitatively documented) source of uncertainty.

A robust quantitative and detailed validation-based estimation of uncertainties of the AEOLUS OC product is not possible due to the small dimension of the comparison dataset.



COLOR

CDOM-proxy retrieval from aeOLus ObseRvations

➤ Introduction

- 1- Scientific context
- 2- COLOR overview

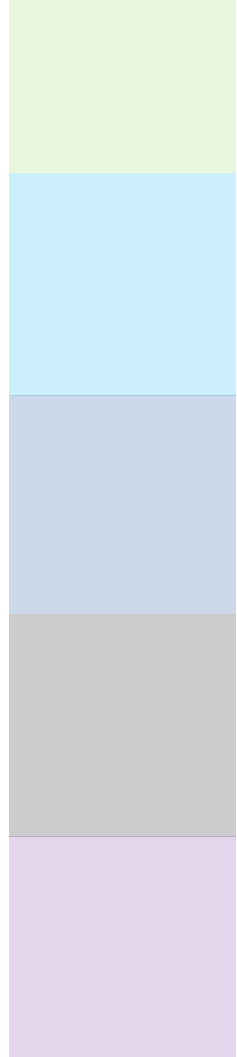
➤ Methods

- 1- LiOC in-water forward model
- 2- AEOLUS in-water algorithm
- 3- AEOLUS data analysis

➤ Results

- 1- Statistical assessment
- 2- Match-up assessment

➤ Roadmap and conclusions





Two different scenarios:

- Scenario 1: optimization of AEOLUS current design and potential improvements for inversion algorithms to achieve the optimal in-water product.
- Scenario 2: applicability of the COLOR results to planned and future satellite missions carrying a lidar that could provide information on oceanic variables.



1 Scenario: Current AEOLUS mission roadmap

Actions to improve the quality of the proposed product:

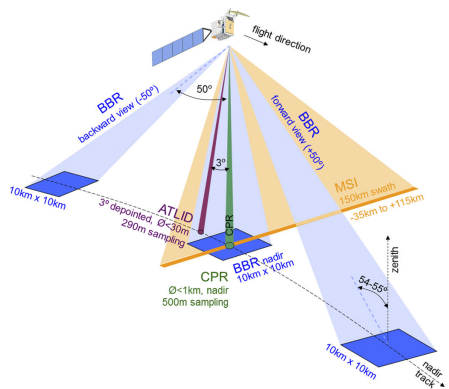
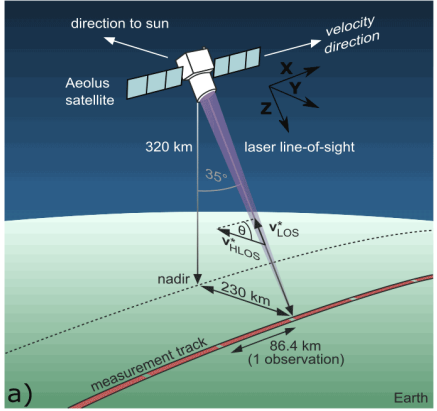
- Improvement in the identification and correction of aerosols and undetected clouds (e.g. L2A product)
- Optimization of the acquisition protocol over the oceans (e.g. reduce the atmospheric portion of the ground bin)
- Exploitation of High Spectral Resolution Lidar (HSRL) capabilities
- Exploitation of the information from other satellite missions (e.g. to improve cloud detection)

Scenario of synergy between satellite missions:

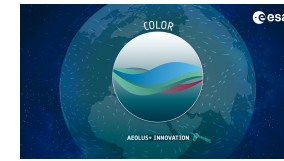
- Inversion algorithm (e.g. variational approach) where active and passive (e.g. MODIS, OLCI) measurements are used as input.

2 Scenario: Applicability of the COLOR results to planned and future satellite missions

Main differences between AEOLUS and ATLID for OC application:



	ALADIN	ATLID	
<input type="checkbox"/> Vertical resolution:	500 m	100 m	Better separation of the atmospheric signal in the ground bin return (e.g. optimization of cloud and aerosols identification)
<input type="checkbox"/> Laser emitting angle:	35°	3°	Stronger surface return and signal propagation
<input type="checkbox"/> Acquisition channels:	-Co-polar Rayleigh A -Co-polar Rayleigh B -Co-polar Mie	-Co-polar Rayleigh -Co-polar Mie -Total cross polar	Optical characterization of the ocean particles through polarization capability
<input type="checkbox"/> Instruments on platform:	-	-Cloud Profiling Radar -Multi-Spectral Imager -Broad-Band Radiometer	Improvement of scene characterization (e.g. cloud detection)
<input type="checkbox"/> Local solar time (LST) sampling:	dawn/dusk	day/night	Large variability of the background signal. Marine diurnal cycle. OC information during nighttime. LST passage closer to OC satellite missions



Development of a status of the art modeling tool (LIOC)

Demonstrated sensitivity of the AEOLUS measurements to marine optical properties

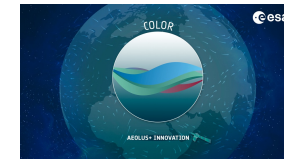
AEOLUS OC prototype product in a spectral region (355 nm) not covered by operational OC products

Overall demonstrated agreement between reference measurements and the proposed OC product

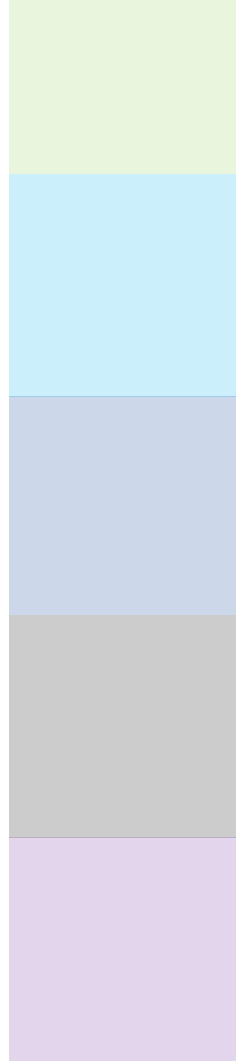
Mission designed for atmospheric wind profiling → In-water profiling capability not available

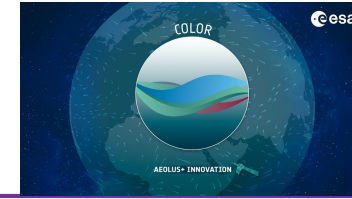
Limited spatial and temporal coverage

Low maturity level of the AEOLUS OC prototype product (e.g. HSRL not exploited, partial associated uncertainties, *home-made* cloud detections and aerosol corrections → Improvements are possible)



- Extend in space (global) and time (all currently available data) the analyses performed and consolidate methodology and results
- Integration of the COLOR results with findings from other relevant AEOLUS studies (e.g. sea surface wind, aerosol products, improved cloud detection)
- Full exploitation of available information (i.e. HSRL capabilities)
- Explore other inversion schemes
- Adapt tools and methodologies to planned/future space lidar missions (e.g. EarthCARE)





CDOM-proxy retrieval from aeOLus Observations

Thanks for your attention

Contact: davide.dionisi@cnr.it

COLOR website: <http://ricerca.ismar.cnr.it/color/>